Thermal and Electrical Conductivities of Dilute Solutions of Iron in Gold†

P. L. Garbarino* and C. A. Reynolds
Physics Department and Institute of Materials Science, University of Connecticut, Storrs, Connecticut 06268
(Received 1 June 1970)

The thermal and electrical conductivities of a specimen of pure gold and 12 dilute gold-iron alloys ranging in iron concentration from 0.01 to 1 at.% have been measured over the temperature range 1–4.2 °K. In addition, the electrical conductivities of six other gold-iron alloys ranging in iron concentration from 0.05 to 2 at.% were measured over the same temperature range. The electrical resistivities of the more dilute specimens exhibit the Kondo logarithmic dependence on temperature; those of the more concentrated samples show the linear dependence on temperature predicted by Harrison and Klein. The data for samples of intermediate concentration show maxima in the resistivity-versus-temperature curve $\rho(T)$. The corresponding temperature T_{max} is found to vary linearly with impurity concentration c. The ratio T_{max}/c is about 24 °K/at.% of iron. The slope of the linear region of $\rho(T)$ varies with the impurity concentration as $c^{1/5}$. A detailed comparison of the dilute-concentration data with Kondo's theory yields a value of $-(0.28 \pm 0.05)$ eV for the s-d exchange energy of gold-iron. The product of the electronic thermal resistivity W_e and the temperature T for the more dilute specimens varies logarithmically with the temperature. The fractional magnitude of the logarithmic term in W_eT is the same as in the electrical resistivity, indicating that, in this range of impurity concentration and temperature, impurity scattering of conduction electrons is predominantly elastic. The Lorenz ratios of these samples are, as a result, independent of temperature, but are a few percent higher than the theoretical Lorenz number L_0. The Lorenz ratios of the more concentrated specimens are found to decrease slowly with decreasing temperature because of the onset of small-angle inelastic conduction-electron scattering. At the upper end of the concentration range, the Lorenz ratio is temperature independent, but depressed by about 15% relative to L_0. The absence of any firm indication of a return of the Lorentz ratio back towards L_0 is discussed in terms of an interaction between an electron and a system of coupled impurities.

I. INTRODUCTION

The effects on the electrical resistivity ρ of exchange scattering of conduction electrons by localized magnetic moments associated with transition impurities dissolved in noble metals have received much attention in recent years.[1] At temperatures low enough so that the resistivity is entirely due to impurity scattering, and for samples sufficiently dilute so that the impurities do not interact with each other, a logarithmic increase of ρ with decreasing temperature T is found experimentally for many members of this class of alloy systems. The logarithmic temperature dependence has been explained by Kondo[2] in terms of exchange scattering by impurity moments whose Zeeman levels are degenerate in energy. His result can be expressed as

$$\rho = \rho_0 + c\rho_m + 3z(c\rho_m)(J/E_F)\ln T\ , \qquad (1)$$

where ρ_0 is the sum of the resistivities due to ordinary potential and non-spin-flip exchange scattering, ρ_m is the spin-flip resistivity per unit fractional impurity concentration, c is the iron concentration, z is the number of conduction electrons per atom, J is the s-d exchange energy, and E_F is the Fermi energy. Kondo's assumption of degenerate Zeeman levels of the impurity moments specifies his result for the case of completely elastic electron scattering.

For more concentrated specimens, the interaction between transition impurities becomes of considerable magnitude, and the degeneracy of the Zeeman levels is lifted. A spin-flip scattering event can, in this case, result in the inelastic scattering of conduction electrons, the difference between incident and scattered electron kinetic energy being the Zeeman energy of the impurity moment, $g\mu_B H$. Here, g is the spin splitting factor, μ_B is the Bohr magneton, and H is the internal field at an impurity site due to the presence of all other transition impurities. The splitting of the Zeeman levels produces a maximum in the electrical resistivity and a subsequent decrease of the resistivity with decreasing temperature.

There have been several models for the internal field H proposed to explain the observed behavior of the resistivity.[3–5] The most sophisticated and the most successful to date has been the model of Klein and Brout[5] as extended by Klein[6] and by Harrison and Klein.[7] They assume a random distribution of impurities all interacting via the short-range Ruderman-Kittel-Yosida[8,9] (RKY) potential. They find that at temperatures well below the resistivity maximum, the resistivity varies linearly with temperature. Their result can be expressed as

$$\rho = \rho_0 + \left(\frac{\Delta\rho}{\Delta T}\right) T \,, \tag{2}$$

where $\Delta\rho/\Delta T$ is the slope of the linear variation. ρ_0 is the resistivity at absolute zero due to ordinary potential and nonflip exchange scattering; the spin-flip resistivity is increasingly "frozen out" as the temperature is decreased toward $T=0$. That is, the Zeeman splitting of the impurity moments becomes progressively greater than the width of the thermal broadening about the Fermi surface $K_B T$. A spin-flip scattering process would require the final state of the electron to be an already occupied state below the Fermi surface; which is, of course, forbidden by the exclusion principle.

The temperature dependencies of the electrical resistivity of gold-iron in the various regions of impurity content have been well established as agreeing with the theories of Kondo and of Harrison and Klein by Gerritsen[10] and by MacDonald *et al.*[11] By measuring 18 samples over three decades of concentration, we studied the concentration dependence of the resistive anomalies as well. In particular, we investigated the concentration dependence of the temperature T_{max} of the maximum in the resistivity-temperature curve. Harrison and Klein propose that T_{max} should be proportional to c. Further, they have found that $\Delta\rho/\Delta T$ is proportional to the excess low-temperature specific heat ΔC_v arising from the ordering of the impurity moments in an internal field, and that both of these quantities are approximately independent of impurity concentration. ΔC_v has been measured in gold-iron by Dreyfus *et al.*[12] who found a weak, approximately $c^{1/5}$, concentration dependence. It will be seen that this same concentration dependence is present also in $\Delta\rho/\Delta T$.

Lutes and Schmit[13] have studied the temperature dependence of the magnetic susceptibility of a 0.5- and a 1-at.% solution of iron in gold. They found broad maxima in the temperature-dependent susceptibilities which are interpreted as being indicative of antiferromagnetic ordering between impurity moments. Lutes and Schmit also found that the temperature of the susceptibility maximum, or the Néel temperature, varied linearly with c and had a value of 8 °K/at.% iron. The value obtained by Klein[6] on the RKY model of the internal field is 7.2 °K/at.%.

A relatively unexplored area is the thermal conductivity of this class of alloy system. To our knowledge, there have been no theoretical predictions as to the effect of inelastic spin-flip exchange scattering on the electronic thermal resistivity W_e. The only experiments have been on the alloy system Ag-Mn,[14,15] and have led to contradictory results.

The total thermal conductivity K of an alloy can be expressed as the sum of an electronic component K_e $(=1/W_e)$ and a component due to heat conduction by phonons K_g:

$$K = K_e + K_g \,. \tag{3}$$

The main source of difficulty in the analysis of the existing data on Ag-Mn lies in the separation of the electronic and phonon conductivities. This difficulty is shared by the present study. However, it will be seen that the number and varying anneal states of specimens included here will enable us to effect the separation by what amounts to the iterative procedure of comparing the lattice conductivity in the various regions of concentration.

In the additive resistance approximation,[16] the lattice (phonon) thermal resistivity W_g $(=1/K_g)$ is

$$W_g = W_E + W_D + W_{pd} \,, \tag{4}$$

where the terms arise from phonon scattering by conduction electrons, dislocations, and point defect associated with the mass difference between solute and solvent, respectively. W_E can be written as $(BT^2)^{-1}$, with B a parameter depending upon impurity concentration; W_D as $(CT^2)^{-1}$, where the quantity C varies linearly with the dislocation density; and W_{pd} as (PT) where P depends on the fractional mass difference between solute and solvent $(\Delta M/M)$ and the impurity concentration c. The similar temperature dependencies of the resistivities due to electrons and dislocations make them almost indistinguishable experimentally. Varying the dislocation density by varying the heat treatment given a sample does, at any rate, provide a method of changing the magnitude of the lattice thermal conductivity.

The electronic thermal resistivity of a nontransition alloy can be written

$$W_e = \beta/T + \alpha' T^2 \,, \tag{5}$$

where the first term arises from impurity scattering, and the second from phonon scattering of conduction electrons. β is a temperature-independent quantity which varies linearly with the impurity content, and α' is a constant. At those temperatures and impurity concentrations, for which the second term in Eq. (5) is negligible with respect to the first, the Lorenz ratio, given by

$$L = \rho/W_e T \,, \tag{6}$$

is a constant in temperature and equal to 2.45×10^{-8} W Ω/°K^2. This is the well-known Wiedemann-Franz law whose applicability is postulated on purely elastic impurity scattering.[17] A channel for small-angle inelastic scattering with electron kinetic energy change of the order of the thermal broadening about the Fermi surface $K_B T$ will increase $W_e T$ relative to ρ with a resulting decrease of L. It is the magnitude, concentration dependence, and temperature dependence of the possible depression of the Lorenz ratio due to inelastic spin-

flip scattering which provided the impetus for the present study.

At this point, some speculation as to the behavior of L in the different ranges of concentration is justifiable since it will aid in a clearer discussion of results. If, in the very dilute specimens, $g\mu_B H$ is much smaller than $K_B T$ and spin-flip scattering is completely elastic, we expect a logarithmically varying term in $W_e T$ analogous to the term in Kondo's result [Eq. (1)]. The fractional magnitude of this logarithmic term should be such as to give a temperature-independent Lorenz ratio that is roughly equal to the elastic scattering value L_0. At intermediate concentrations where the internal field becomes of such magnitude that

$$g\mu_B H \sim K_B T \,, \tag{7}$$

spin-flip scattering will take on an inelastic character. If the exchange scattering is of sufficiently small angle, a depression of the Lorenz ratio will ensue. At a low enough temperature or high enough concentration, such that

$$g\mu_B H \gg K_B T \,, \tag{8}$$

a significant portion of the inelastic spin-flip processes will be "frozen out" of the resistivities, and a rise in L back towards its elastic scattering value is foreseen. At $T = 0\,^{\circ}\mathrm{K}$, this freezing-out process will be complete and L must again equal L_0. Here, as elsewhere in this paper, "dilute" is taken to mean of low enough concentration that conduction-electron scattering is completely elastic; "intermediate" as that concentration domain in which some of the scattering becomes inelastic; and "concentrated" as that impurity range in which inelastic scattering is well on its way to being frozen out. These correspond to the concentration ranges 0–0.03, 0.03–0.15 at.%, and greater than 0.15 at.%, respectively, for the range of temperature studied.

II. EXPERIMENTAL PROCEDURES AND APPARATUS

A. Sample Characteristics and Treatment

The alloys used in this experiment can be classified into two sets. The first, [18] designated as "Au" alloys, were prepared by melting together, under vacuum, the proper amounts of gold and iron in high-purity graphite crucibles. The purity of the starting materials was specified to 99.999% or better. The alloy ingots thus prepared were cold rolled and drawn to wires of approximately 0.040-in. diameter. The second, [19] designated as "Au_b" alloys, were prepared from starting materials of unknown purity in an argon arc furnace and drawn into wires of about 0.010-in. diameter.

Spectroscopic analysis for trace amounts of unwanted metallic impurity was performed on both sets of alloys. For the "Au" set, the total unwanted impurity content was less than 0.001% in all cases; for the "Au_b" set less than 0.05% for each alloy except the most concentrated alloy (1.92 at.% of Fe) which contained 0.15 at.% of spurious impurity. In all cases, the major unwanted impurities were Cu, Ag, Si, and Pb; only trace amounts of transition elements besides iron were found in the finished alloys.

Samples of roughly 17-cm length were cut from the unannealed alloy wires, and all samples within the Au set, except for two which will be discussed later, were subjected to an annealing study in the following manner. The electrical resistivity at 4.2 °K of each sample was measured both before and after a 36-h anneal at 600 °C. Annealing was accomplished under vacuum (less than 1 Torr) in sealed Vycor tubes. As shown in Table I, the resistivities after anneal were systematically less than those before anneal by about 0.5–0.9 $\mu\Omega$ cm. Since the heat treatment had the additional effect of making the rigid "as-received" wires soft and limp, this decrease in resistivity is attributed to an elimination of a large fraction of the lattice defects created during the drawing process of sample fabrication. This explanation is reinforced by a sharp reduction of the lattice thermal conductivity due to the presence of a large dislocation density in the unannealed specimen (see Sec. III B). The absence of any further resistivity change of selected specimens on an additional 36-h anneal at 600 °C leads us to conclude that 36 h is sufficient to realize a homogeneous distribution of impurity over the cross-sectional area of the specimen and to eliminate a large fraction of the lattice defects.

Because of the fragile nature of the "Au_b" set of samples, the annealing study was confined to the "Au" set of samples. In fact, it was found that the "Au_b" set was too thin to perform the experimental mechanics of thermal conductivity on. Measurement of this set was therefore confined to electrical resistivity. The "Au_b" set of samples was given a 36-h anneal at 600 °C as is indicated in Table I.

It is also seen in Table I that samples cut from a particular alloy set are named via two numbers. The first number refers to the alloy the sample was cut from and therefore indicates composition. The second indicates the number sample cut from a particular alloy. For example, Au 3-2 means the second sample cut from alloy number three (0.0273 at.%) of the "Au" set.

Homogeneity of impurity distribution along the length of the specimens of both sets was checked by measuring the 4.2 °K resistivity of different segments of the sample. In no case was any measurable impurity gradient detected. The resolution of this particular measurement was about 0.5%.

B. Impurity Concentration Determination

The impurity concentrations quoted in Table I

were found by plotting the resistivity ratio r, defined by

$$r = \rho_{4.2}/(\rho_{273} - \rho_{4.2}) , \quad (9)$$

against the nominal concentration and the concentration found by spectrographic and/or chemical analysis, the results of which were supplied with the alloys. This plot is shown in Fig. 1. The solid curve is felt to be the most representative of all the data. That value of the abscissa corresponding to the measured resistivity ratio as read from the curve was then taken to be the actual impurity concentration. Values of c thus obtained are uncertain to no more than ± 2%.

C. Method of Measurement

Electrical resistivity measurements were accomplished with the sample in direct contact with the liquid-helium bath by a standard four-terminal dc potentiometric technique. The instrumentation and procedure have been previously described in detail by Burckbuchler and Reynolds.[20] Resistivity changes of typically 0.02% could be detected with this apparatus. Uncertainties in the measurement of geometrical factors associated with resistivity measurement introduce an uncertainty of approximately 1% into the specification of the magnitude of a resistivity. At all points during the experiment, the temperature of the liquid-helium bath was found from the 1958 He vapor-pressure tables. The uncertainty in temperature measurement is estimated to be less than 0.001 °K.

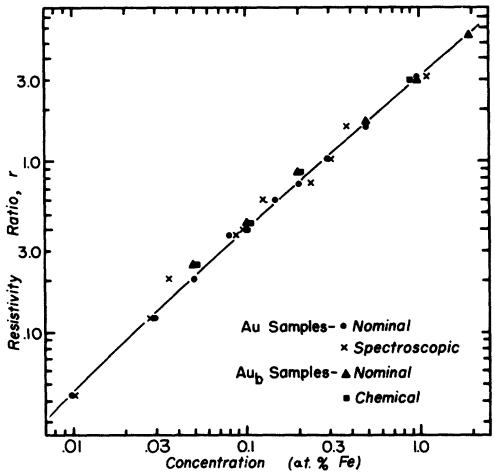

FIG. 1. Plot of the resistivity ratio against nominal impurity concentration and impurity concentration as found by spectroscopic or chemical analysis. The solid line is felt to be best representative of all the data. The solid line and the measured resistivity ratios are then used to determine the "actual" impurity concentration.

The method of germanium-resistance thermometer calibration and thermal-conductivity measurement has been discussed in sufficient detail by Gueths *et al.*[21] Our procedures differ from those of Gueths in two important respects. (i) A Hewlett Packard model No. 2411A guarded dc amplifier along

TABLE I. Sample resistivities[a] at 273, 77, and 4.2 °K.

Sample	Concentration[b] (Deduced)	4.2[c] (0 h)[d]	4.2[c] (36 h)[d]	4.2[c] (72 h)[d]	77[c]	273[c]	r[e]
Au 1-1	Pure	0.0159	...	0.0038	0.440	2.045	0.001 865
Au 2-1	0.0091	0.1312	0.0852	0.0852	0.527	2.109	0.0421
Au 3-1	0.0273	0.3047	0.2471	...	0.695	2.269	0.1222
Au 3-2[f]	0.0273	0.300	...	...	0.732	0.295	0.1504
Au 4-1	0.047	0.466	0.408	...	0.862	2.435	0.2012
Au 5-1	0.091	0.830	0.765	...	1.231	2.812	0.3733
Au 6-1	0.096	0.850	0.786	0.786	1.251	2.828	0.3847
Au 7-1	0.153	1.279	1.212	...	1.692	3.280	0.5859
Au 8-1	0.193	1.595	1.523	...	2.016	3.602	0.7323
Au 9-1	0.282	2.21	2.15	...	2.664	4.25	1.019
Au 10-1	0.460	3.48	3.42	...	4.003	5.60	1.573
Au 11-1	0.98	7.47	7.47	7.47	8.24	9.82	3.174
Au 11-2[f]	0.98	7.51	...	...	8.25	9.83	3.237
Au$_b$ 1-1	0.50	...	3.760	...	4.39	5.99	1.686
Au$_b$ 2-1	0.91	...	6.73	...	7.45	9.03	2.923
Au$_b$ 3-1	1.92	...	14.63	...	15.78	17.40	5.284
Au$_b$ 4-1	0.056	...	0.487	...	0.938	2.48	0.2444
Au$_b$ 5-1	0.106	...	0.8822	...	1.356	2.92	0.4333
Au$_b$ 6-1	0.230	...	1.770	...	2.267	3.84	0.8538

[a] All resistivities in μΩ cm.

[b] Concentrations as found from the solid line in Fig. 1.

[c] Numbers refer to temperature at which resistivity measurement was performed in °K.

[d] Times refer to length of anneal before resistivity measurement.

[e] The resistivity ratio; $r = \rho_{4.2}/(\rho_{273} - \rho_{4.2})$.

[f] Unannealed specimen.

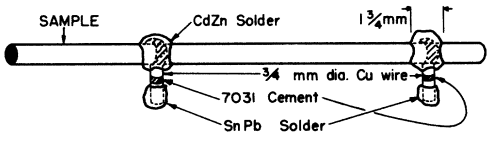

FIG. 2. Details of copper-sleeve attachment to the sample. Use of these sleeves for both potential and thermal contact to the sample ensures that the geometrical factors are the same for both types of measurement.

with a 1-μV least-count digital voltmeter (either a Honeywell model No. 630S or a Hewlett Packard model No. 2401B) was applied to the measurement of potential drop across the thermometers. The amplifier is capable of being operated in either a +1 or +10 gain mode. The amplifier-digital voltmeter combination provides a voltage measuring device the usefulness of which is based on (a) an input impedance (10^{10} Ω) a factor of 10^5 higher than that of the digital voltmeter alone; (b) a least count of 0.1 and 1 μV when operated in the +10 and +1 gain modes, respectively; (c) an acceptably low level of noise; and (d) a gain accuracy of 0.007 and 0.002% for a +10 and +1 gain, respectively. Over the temperature range 4.2—1.5 °K and at a measuring current of approximately 0.5 μA, the resistance of a germanium-resistance thermometer varies from 1 to 50 °KΩ, and the sensitivity dR/dT varies from 1500 to 50 000 Ω/°K. The high input impedance of the amplifier-digital voltmeter combination is necessary to make loading effects negligible. The least-count and low noise level enable detection of temperature changes of 1 mdeg or less over the entire temperature range. The chief advantage of the amplifier-digital voltmeter combination over the older potentiometric method of voltage measurement is that the speed of data acquisition is increased by about a factor of 10. Much of the tedium involved in the use of a potentiometer is avoided. Elimination of errors due to the unavoidable drifts in the temperature of the liquid-helium refrigerant, resultant to this increased speed, enables higher-quality thermal-conductivity data to be obtained as well. (ii) The details of the method of potential and thermal contact to the sample are shown in Fig. 2. Copper sleeves were soldered directly onto the sample with an alloy composed of 82% Cd and 18% Zn.[22] As was verified experimentally, this solder does not superconduct in the liquid-helium range of temperatures. Potential leads or thermometers were in turn fastened to the sleeves with Sn-Pb solder. Since Sn-Pb solder melts at a lower temperature than Cd-Zn, this joint could easily be made without melting the Cd-Zn. The GE 7031 cement shown between solder joints served only to dirty the surface of the sleeve ensuring that the Sn-Pb could not run onto Cd-Zn. In this manner, it was ensured that the geometrical factors were the same for both thermal and electrical measurement and that the uncertainties would cancel in the Lorenz ratio ρ/W_eT. The distance between sleeves ranged from 10 cm for the pure-gold specimen down to 4 cm for the most concentrated sample.

III. RESULTS

A. Electrical Resistivity

Representative electrical resistivity data for the very dilute specimens are plotted against the logarithm of the temperature in Fig. 3. The numbers in parentheses are the impurity concentrations in at.%. The straight lines represent the results of least-squares fits of the data to the Kondo logarithmic variation

$$\rho = A + D\ln T\,, \tag{10}$$

with A and D temperature-independent constants. The values of A and D are listed in Table II along with values found by MacDonald *et al.*[11] The impurity concentrations quoted for MacDonald's samples were found using the reported resistivity ratios and our resistivity-ratio data (Fig. 1). The numbers in parentheses beneath these determined concentrations are the nominal concentrations of his samples.

Figure 4 shows representative electrical resistivity data for intermediate-concentration samples which exhibited maxima in the temperature range studied. The temperatures at which the maxima occur, T_{max}, are shown plotted against im-

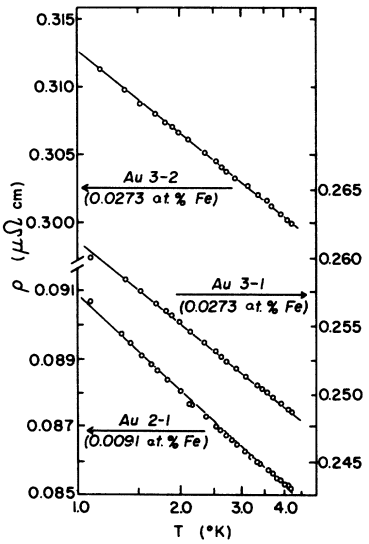

FIG. 3. Logarithmic temperature variation of the resistivity for the three most dilute samples. Numbers in parentheses are the impurity concentrations in at.%. Straight lines represent the results of a least-squares fit to the data to the Kondo logarithmic variation. Sample Au 3-2 is unannealed specimen.

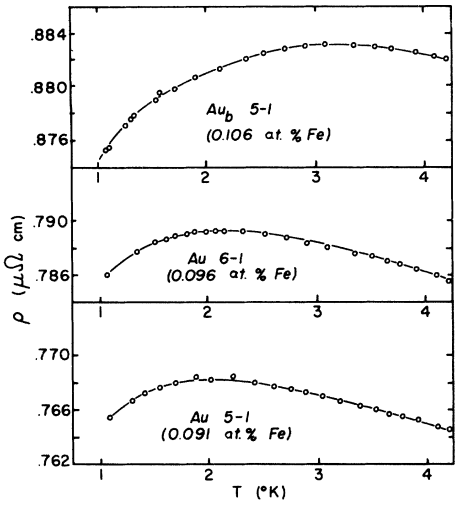

FIG. 4. Representative electrical resistivity data for samples in the intermediate concentration range. Numbers in parentheses are the impurity concentrations in at.%.

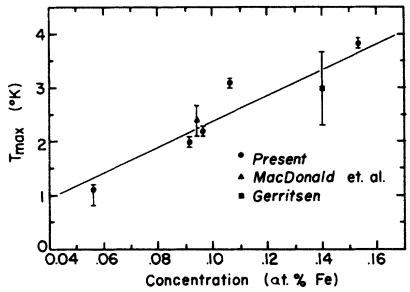

FIG. 5. Temperature at which the resistivity passes through a maximum T_{max} plotted against impurity concentration. A least-squares fit of all the data to a linear concentration dependence of T_{max} gives $T_{max}/c = 24$ °K/at.%. The solid line is representative of this least-squares fit.

purity concentration in Fig. 5. The solid triangle and solid square are the results of MacDonald *et al.* and of Gerritsen.[10] Although the data are somewhat scattered, the linear dependence predicted by Harrison and Klein is indicated. The solid line represents the result of a least-squares fit of all the data to a linear variation. The fit gives

$$T_{max}/c = 24\,^{\circ}\mathrm{K/at.\,\%}\,. \tag{11}$$

Figure 6 shows representative electrical resistivity data for the high-impurity concentration specimens. The solid lines represent the results of least-squares fits of the data to the linear variation of resistivity with temperature [Eq. (2)].

Values of the slope $\Delta\rho/\Delta T$ of the linear region of the resistivity-versus-temperature curve and extrapolated values of the resistivity at absolute zero were found for each of the more highly concentrated specimens. These values are listed in Table III. Figure 7(a) is $\Delta\rho/\Delta T$ plotted against impurity concentration on logarithmic scales. The data show that

$$\Delta\rho/\Delta T \sim c^{1/5}\,. \tag{12}$$

This slow variation with concentration correlates well with the approximately $c^{1/5}$ concentration dependence of the excess low-temperature specific heat ΔC_v found by Dreyfus *et al.*[12] and with the relationship between ΔC_v and $\Delta\rho/\Delta T$ proposed by Harrison and Klein.

Figure 7(b) is a plot of the extrapolated values of the resistivity at absolute zero against impurity concentration. ρ_0 varies linearly with concentration, and is 7.5 ± 0.1 $\mu\Omega$ cm/at.% of impurity. ρ_0, the temperature-independent contribution of ordinary potential and nonflip exchange scattering can be found for the very dilute specimens by multiplying the determined impurity concentration by this value. These values of ρ_0 and of the quantity $A - \rho_0$, which, by comparison of Eqs. (1) and (8), is the temperature-independent spin-flip resistivity $c\rho_m$, are listed in Table II. Then $c\rho_m$ is eliminated as an unknown from the coefficient of the logarithmic term, and we have

$$B = 3z(c\rho_m)J/E_F\,. \tag{13}$$

Taking z, the number of conduction electrons per atom, to be one[23] and E_F, the Fermi energy, to be the free-electron value[2] of 5.5 eV yields a value of J. These are listed in the last column of Table

TABLE II. Temperature-dependent resistivity characteristics of very dilute specimens.

Sample	Concentration (at.%)	A ($\mu\Omega$ cm)	D ($\mu\Omega$ cm)	ρ_0 ($\mu\Omega$ cm)	$A-\rho$ ($\mu\Omega$ cm)	J (eV)
Au 2-1	0.0091	0.0908	-4.03×10^{-3}	0.068	0.023	-0.32 ± 0.06
Au 3-1	0.0273	0.261	-8.57×10^{-3}	0.204	0.057	-0.27 ± 0.03
Au 3-2[a]	0.0273	0.312	-8.67×10^{-3}	...	...	...
Au M-1[b]	0.0073 (0.006)	0.077	-4×10^{-3}	0.054	0.022	-0.33 ± 0.08
Au M-2[b]	0.020 (0.02)	0.2	-7.8×10^{-3}	0.15	0.050	-0.29 ± 0.04

[a]Unannealed specimen.

[b]Results of MacDonald *et al.* (Ref. 11).

II. The best value of J obtainable from our data, combined with that of MacDonald, is

$$J = -(0.28 \pm 0.05)\ \text{eV} . \quad (14)$$

We are not aware of any previous determination of J for the gold-iron system. Our value, however, appears to be of reasonable magnitude.[2]

Tables II and III show that the values of the slope of the linear region of the resistivity-temperature curve and of the coefficient of the logarithmic term are similar for the annealed and unannealed samples of the same impurity concentration. The only difference in their properties is that there is an additional temperature-independent contribution to the resistivity which, as in the discussion of Sec. II, is attributable to electron scattering by lattice defects. This is evidence that the state of anneal has no effect on the spin-flip scattering responsible for the resistive anomalies. The annealed and unannealed samples were cut from adjacent segments of the same batch of alloy material; to draw definite conclusions as to the effect of the state of anneal on the resistive anomalies, measurements should be performed on the same sample both before and after anneal. Our procedure of solder contact to the sample precluded this course of action.

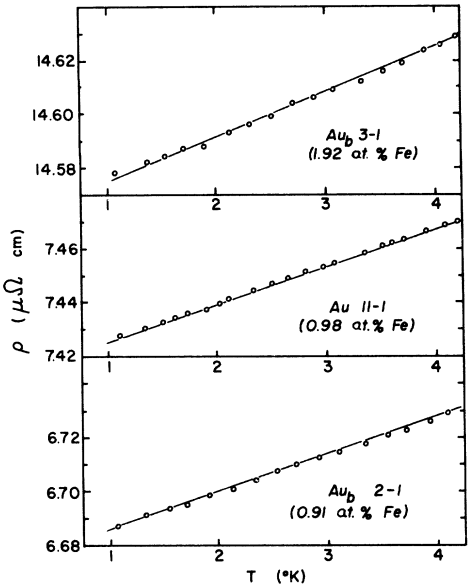

FIG. 6. Representative electrical resistivity data for the most highly concentrated samples. Numbers in parentheses are the impurity concentrations in at.%. Solid lines are the results of a least-squares fit of the data to the linear dependence predicted by Harrison and Klein.

B. Thermal Conductivity

The thermal-conductivity data of the pure-gold specimen are displayed in Fig. 8 as a plot of the thermal resistivity $W_e T$ (in this case, the fractional magnitude of the lattice conductivity is small enough to be neglected) against T^3. The data are well described by Eq. (5) written as

$$W_e T = \beta + \alpha' T^3 . \quad (15)$$

The slope of the straight line gives a value of 1.6×10^{-4} cm/°K W for the parameter α'. This is to be compared with 1.8×10^{-4} and 1.3×10^{-4} cm/°K W found by Rosenberg[24] and by White,[25] respectively, on gold of comparable purity.

TABLE III. Temperature-dependent resistivity characteristics of more highly concentrated specimens.

Sample	Concentration (at.%)	ρ_0 (μΩ cm)	$\Delta\rho/\Delta T$ (μΩ cm/°K)
Au 7-1	0.153	1.188	1.02×10^{-2}
Au_b 8-1	0.108	1.493	1.06
Au_b 6-1	0.230	1.734	1.01
Au 9-1	0.282	2.107	1.18
Au 10-1	0.460	3.375	1.27
Au_b 1-1	0.50	3.714	1.21
Au_b 2-1	0.91	6.673	1.38
Au 11-1	0.98	7.412	1.39
Au 11-2[a]	0.98	7.455	1.41
Au_b 3-1	1.92	14.56	1.68

[a]Unannealed specimen.

Figure 9 is a plot of the Lorenz ratio against temperature for the pure-gold specimen. The experimental points were found by dividing the measured resistivities (which were found to be temperature independent) by $W_e T$ read from the line in Fig. 8. The depression of the Lorenz ratio at higher temperatures is attributed to small-angle inelastic scattering of electrons by phonons. At the lowest temperature of measurement, the Lorenz ratio is 2.48 ± 0.06 W Ω/°K^2.

Figure 10 shows representative thermal-conductivity data for the very dilute alloy specimens, displayed as plots of the total thermal conductivity K, divided by the temperature against the temperature. For nontransition alloys in those cases where the phonon term T^2 in the electronic thermal resistivity is negligibly small (as it is for all of our alloy specimens), the quantity K/T is expected to depend linearly on temperature according to the prescription

$$K/T = 1/\beta + BT . \quad (16)$$

The significant deviations to the linear behavior evident in the data in Fig. 10 will be shown to be the result of spin-flip exchange scattering on the electronic thermal resistivity.

Representative data for the more highly concentrated alloys are shown in Fig. 11. The good fit of the data to a linear variation of Eq. (10) indicates

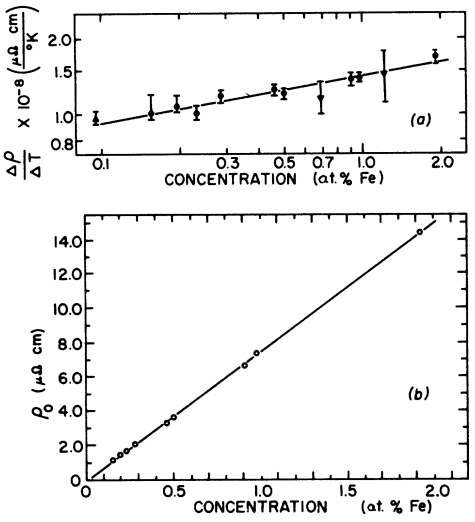

FIG. 7. (a) $\Delta\rho/\Delta T$ vs c for those samples which showed a linear $\rho(T)$ above 1 °K. The values of $\Delta\rho/\Delta T$ shown were obtained directly from least-squares fits like those in Fig. 6. The triangle and inverted triangle are values of $\Delta\rho/\Delta T$ deduced from the published data of MacDonald *et al.* and of Gerritsen, respectively. (b) Extrapolated values of the resistivity at absolute zero ρ_0 vs concentration. Here, as in (a), values of ρ_0 were obtained from least-squares fits and could be obtained only for concentrated specimens.

that spin-flip effects are slowly varying with temperature enough so as to be obscured by the large fractional magnitude of the lattice conductivity.

The fractional contribution of the lattice conductivity BT^2 to the total conductivity K ranged from 4%, for the most dilute specimen, up to 50% for the most concentrated, and so was non-negligible for all samples. In the higher ranges of impurity content, the magnitude of the lattice conductivity was estimated by using plots like those in Fig. 11 to determine the coefficients B of the T^2 variation of the lattice conductivity. These are plotted against impurity concentration as the solid circles in Fig. 12. The solid triangle is a previous result of White *et al.*,[26] and the solid diamond is an estimate of the value of B for the pure-gold specimen made from our experimental value of the parameter α and the relation between these two quantities derived by Klemens.[27] The values of the lattice conductivities for samples in the dilute-concentration range are estimated by an extrapolation of the higher-concentration results. This extrapolation is shown as the dashed line in Fig. 12. The significance of the solid squares will be discussed shortly.

In this manner, values of the coefficient B, and hence of the magnitude of the lattice conductivity, could be found over the entire concentration range. According to Eq. (3), the electronic thermal conductivity is then isolated as the difference between the total measured conductivity and the lattice conductivity. However, a calculation of the thermal resistivity due to mass defects associated with impurity ions has shown that this procedure overestimates the lattice conductivity for the most highly concentrated samples (density-of-mass defects largest). That is, the phonon scattering by mass defects decreases the lattice conductivity slightly in the four most concentrated samples, the maximum reduction being 2% of the lattice conductivity for the 0.98-at.% sample. For these samples, the lattice conductivity was calculated from the estimated value of B and the expression[28]

$$K_g = BT^2[I(\alpha)/7.21] , \tag{17}$$

with

$$I(\alpha) = \int_0^\infty \frac{x^3 e^x}{(e^x-1)^2} \frac{dx}{1+\alpha x^3} . \tag{18}$$

The parameter α is given by

$$\alpha = \frac{\pi^2 a^3}{7.21 V_T h} \left(\frac{\Delta M}{M}\right) B_c T^3 , \tag{19}$$

where a^3 is the volume per atom (1.7×10^{-28} cm^3 for gold), V_T is the transverse sound velocity in gold (1200 m/sec), and h is Planck's constant. It is seen that Eq. (16) correctly reduces to BT^2 in the limit of vanishing defect concentration c, since for $\alpha = 0$, $I(\alpha)$ is just the well-known transport integral $J_3(\infty) = 7.21$.[29]

For the very dilute specimens, values of $W_e T$ ($= T/K_e$) resulting from the separation of the con-

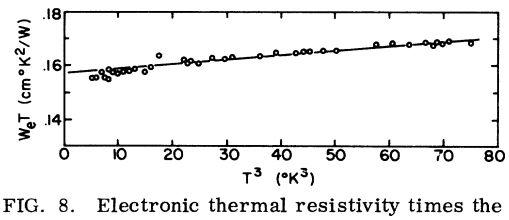

FIG. 8. Electronic thermal resistivity times the temperature against the cube of the temperature. The slope of the solid line gives the value of α' in Eq. (15) to be 1.6×10^{-4} cm/°K W.

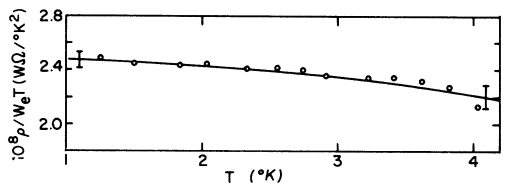

FIG. 9. Lorenz ratio of the pure-gold specimen. Error bars at the extremities of the temperature range indicate the uncertainty due primarily to scatter in the data. At the lowest temperature of measurement, L is 2.48 ± 0.06 WΩ/°K^2.

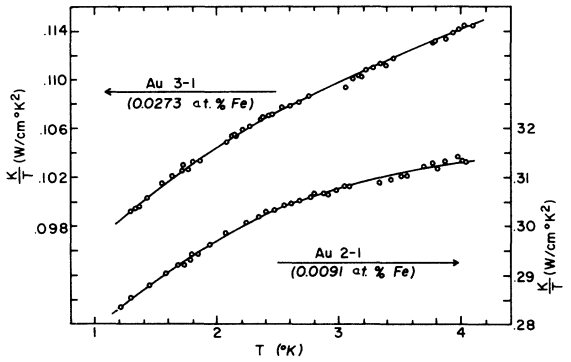

FIG. 10. Representative thermal-conductivity data for very dilute-alloy specimens displayed as plots of K/T against T. Numbers in parentheses are the impurity concentrations in at.%.

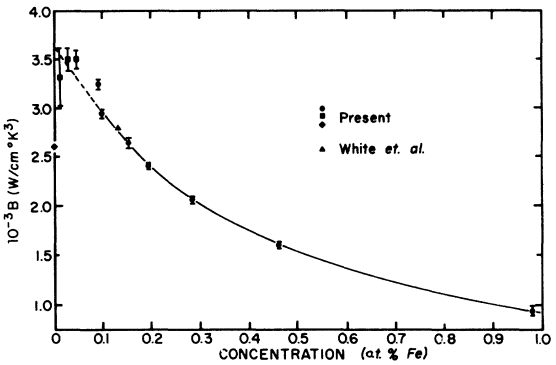

FIG. 12. Values of B, the coefficient of the T^2 term in the lattice conductivity, plotted against impurity concentration. Solid circles result from a fit of the data to Eq. (16). The solid diamond is an estimate of B for the pure-gold specimen made from the experimental value of the parameter K and the theory of Klemens (Ref. 27). The solid triangle is the result of White *et al.* (Ref. 26). The dashed line segment represents an extrapolation of the high-concentration results into the very dilute range. Solid squares are values of B obtained by eliminating the effect of spin-flip exchange scattering in the dilute-concentration data, using the results of resistivity measurement.

ductivities were found to depend logarithmically on the temperature, as is shown in Fig. 13. The data for the four samples considered were fitted to the equation

$$W_e T = \beta + Q \ln T , \tag{20}$$

and a quantitative comparison was made with the results of resistivity measurement by comparing the ratios $|Q|/\beta$ and $|D|/A$. Q and β are just constants. A and D are constants obtained from the fit of the resistivity data to Eq. (10), as previously discussed. Values of these ratios are listed in Table IV. The limits of error quoted are primarily caused by the uncertainty in estimating the magnitude of the lattice conductivity. The values of the ratios for each sample are seen to be in good agreement, indicating that spin-flip scattering of conduction electrons by localized moments is equally effective in the thermal and electrical resistivities. For the reasons discussed in Sec. I, this means that, in this range of temperature and concentration, spin-flip scattering is predominantly elastic, consistent with the assumption of Kondo.

The electrical resistivity data for sample Au 4-1 exhibit, at the lowest temperatures of measurement, slight deviations from a logarithmic dependence on temperature. This deviation is ascribable to the onset of the resistivity maximum but results in an uncertainty in the value of $|D|/A$, as is in-

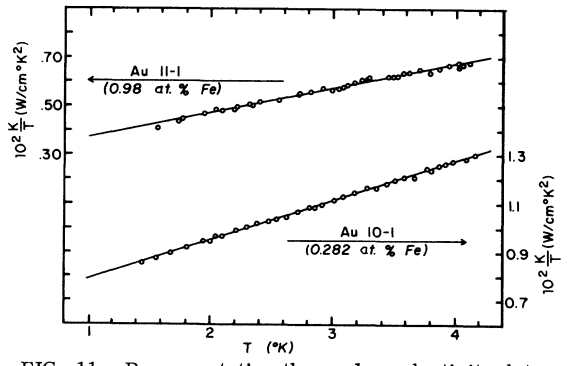

FIG. 11. Representative thermal-conductivity data for the most highly concentrated specimens displayed as plots of K/T against T. Numbers in parentheses are the impurity concentrations in at. %.

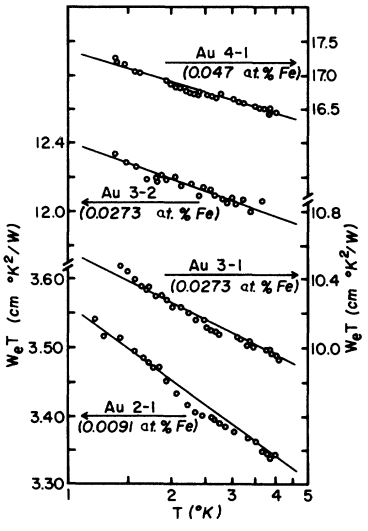

FIG. 13. Plots of the electronic thermal resistivity times the temperature against the temperature for the four most dilute specimens. Solid lines are the result of a fit of the data to Eq. (20).

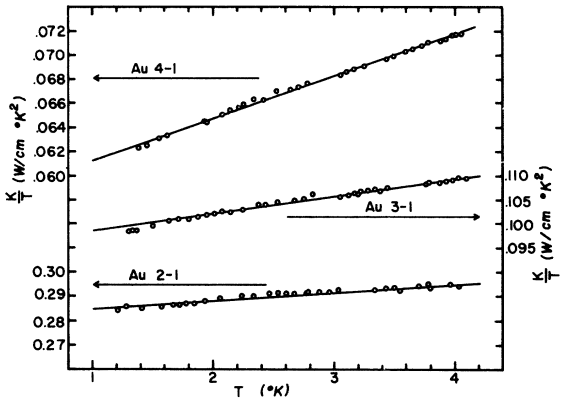

FIG. 14. Values of the total thermal conductivity divided by the temperature against the temperature corrected for the effects of spin-flip exchange scattering by a method described in the text. The data describe straight lines as would be expected for a T^2 variation of the lattice thermal conductivity. The slopes of these lines yield values of B which are shown as the solid circle in Fig. 12.

dicated in Table IV. This observation correlates with the slightly larger magnitude of $|Q|/\beta$ relative to $|D|/A$ evident in Table IV for this sample. The effect of a small admixture of inelastic scattering would be to cause a deviation in the values of the ratios in the above-noted sense.

The consistency of the analysis to this point can be demonstrated in the following manner. Starting with the conclusion of equal effect of spin-flip processes on the two resistivities, the values of D/A (obtained from the resistivity data) are used to eliminate the logarithmic exchange-effect induced term in the *total* thermal resistivity according to the prescription

$$(WT)_c = WT[1 - (|D|/A)\ln T] . \quad (21)$$

The effect of subtracting the logarithmic term from the total thermal resistivity, and not just the electronic part, is to introduce an error of the order of $|D|/A$ times the fractional magnitude of the lattice conductivity. This error is at worst 0.3%, and is therefore negligible. Figure 14 exhibits the values of K/T $[=1/(WT)_c]$ obtained in this manner. The slopes of the straight lines yield values of the parameter B. These values of B are shown plotted as the solid squares in Fig. 12. The agreement with the original extrapolation (dashed line segment) is good.

TABLE IV. Comparison of the logarithmic increases in $\rho(T)$ and W_eT.

Sample	Lattice fraction[a]	β (cm °K^2/W)	$\lvert Q\rvert/\beta\times10^2$	$\lvert D\rvert/A\times10^2$
Au 2-1	0.04	3.56	4.5±0.3	4.43±0.04
Au 3-1	0.10	10.6	4.0±0.8	3.28±0.03
Au 3-2[b]	0.02	12.4	2.5±0.5	2.78±0.06
Au 4-1	0.15	17.3	3.6±1.0	2.39±0.10

[a]Fraction of lattice conductivity.
[b]Unannealed specimen.

There is to be found some support for our conclusion regarding the equal efficacy of exchange scattering on the electronic thermal and electrical resistivities in the work of Spohr and Webber.[30] They observe (i) for a Mg-Mn alloy (of electrical resistivity 0.15 $\mu\Omega$ cm at 1 °K), equal effects of exchange scattering on the two resistivities; and (ii) for a Mg-Fe sample (of electrical resistivity 0.06 $\mu\Omega$ cm at 1 °K) an anomalously high lattice thermal conductivity of fractional magnitude 0.04. Given a significant lattice conductivity in the material of lower electrical resistivity, we would expect to find one in the material of higher electrical resistivity as well. No account of the possible contribution of K_g was taken by Spohr and Webber in the analysis of the data for the Mn-doped specimen since the data, by which they could do so, were lacking for more concentrated alloys. From their experimental value of α and the theoretical relationship of Klemens,[28] we have calculated that K_g should be only 0.5% of K_e for the Mn-doped specimen and correspondingly less for the other sample. Therefore, we feel that their results, at least for the Mn-doped sample, are in substantial agreement with ours, but we must leave the anomalously high thermal conductivity they observed for the Mg-Fe sample unexplained.

C. Lorenz Ratio

Figure 15 is a plot of the Lorenz ratio against temperature for all samples upon which thermal-conductivity measurement was performed. The numbers in parentheses give the impurity concen-

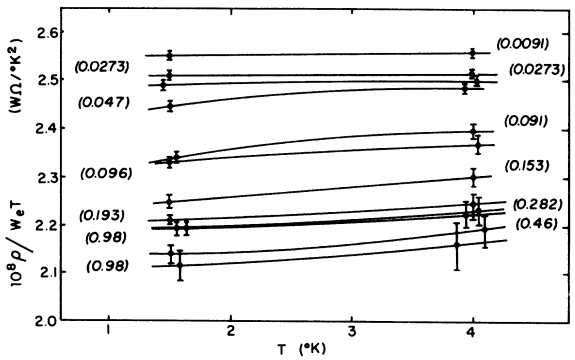

FIG. 15. Lorenz ratio plotted against temperature. Numbers in parentheses refer to the impurity concentration of the sample at at.%. Error bars indicate the uncertainty in temperature variation, due mainly to the fractional size of the lattice conductivity.

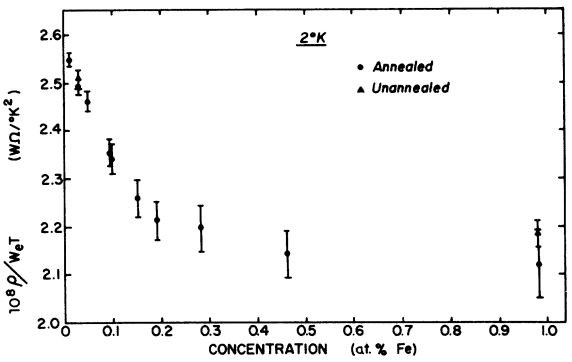

FIG. 16. Lorenz ratio at 2 °K plotted against the impurity concentration. The results for the annealed specimens are shown as solid circles; those for the unannealed as solid triangles. Error bars indicate the experimental uncertainty and are primarily resultant upon the separation of the electronic thermal conductivity from that of the lattice.

tration of that sample in at. %. The error bars at the beginning and end of the temperature range of measurement indicate the uncertainty in the temperature dependence of the Lorenz ratio. This uncertainty arises mainly from the separation of lattice and electronic conductivities. Figure 16 is a plot of the Lorenz ratio as a function of impurity concentration at the fixed temperature of 2 °K. In this case, the error bars indicate the uncertainty in the magnitude of the Lorenz ratio and, again, are primarily resultant to inaccuracies inherent in separating the conductivities. In both curves the uncertainties increase with the fractional magnitude of the lattice conductivity.

For the three most dilute specimens, the Lorenz ratio is constant in the temperature. This is a result of the predominantly elastic nature of the exchange scattering in this region of temperature and impurity concentration, as was discussed in Sec. III B. However, the value of the Lorenz ratio is 4% higher than the theoretical Lorenz number. It is unlikely, in view of the smaller fractional magnitude of the lattice thermal conductivity of pure substances and very dilute alloys, that this slightly high value of the Lorenz ratio could be caused by an underestimation of the lattice conductivity.

A noticeable decrease of the Lorenz ratio with decreasing temperature is first evident for the 0.047-at. % specimen (sample Au 4-1). This correlates well with the observation of small deviations to the Kondo $-\ln T$ behavior in the resistivity of this specimen.

An interesting feature of Fig. 15 is that in the higher-concentration ranges, where the depression of the Lorenz ratio is greatest, there is as yet no indication of a trend in the temperature-dependent Lorenz number back towards the theoretical Lorenz ratio. This is surprising, because 4 °K is already one-half of the Néel temperature of the 0.98-at. % alloy.[13] In view of the size of the uncertainties, the Lorenz ratio may be taken to be independent of T in the high range of impurity concentration.

IV. DISCUSSION

Phenomenologically the depression of the Lorenz ratio $1 - L/L_0$ is proportional to the probability P of inelastic spin-flip scattering times the number N of local moments in fields $\mu_B H \lesssim K_B T$ divided by the amount of elastic scattering (which is proportional to the resistivity due to elastic scattering ρ_e). N depends on the temperature and on the concentration; we will assume P to depend only on temperature. P_e varies only slowly with temperature and approximately linearly with concentration. That is,

$$1 - \frac{L}{L_0} \to \left(1 - \frac{L}{L_0}\right)^2 \sim \frac{P(T)N(T, c)}{P_e(c)} . \tag{22}$$

The constant behavior of the temperature-dependent Lorenz ratio for high-concentration specimens indicates that the product of $P(T)$ and $N(T, c)$ is constant in temperature. The temperature dependence of N reflects the shape and temperature dependence of the probability distribution $P(H)$ of internal fields. Harrison and Klein have calculated the probability of inelastic spin-flip processes and found that it goes to zero exponentially in the asymptotic limit of high fields and low temperatures. Unless $N(T, c)$ increases almost as rapidly in the asymptotic limit, it can be said that 1.5 °K is not a sufficiently low temperature to reach the asymptotic region for an impurity concentration of 0.98 at.%. However, 1.5 °K is one-fifth of the Néel temperature of such an alloy. A continuation of the experiment in a He^3 refrigerator would, therefore, be likely to reveal further information in this connection.

Figure 16 shows that the Lorenz ratio at 2 °K decreases rapidly with increasing impurity content to a concentration of about 0.2 at.%. At that point, it ceases its decline and remains approximately constant to the upper end of the concentration range. 0.2 at.% corresponds (according to the results of Lutes and Schmit[13]) to that impurity concentration necessary for an alloy to exhibit a Néel temperature in the liquid-helium range. According to Eq. (22), the rapid decrease of the isothermal Lorenz ratio at concentrations less than 0.2 at.% indicates that $N(T, c)$ varies more rapidly than linearly with concentration in this range. The subsequent constancy of the isothermal Lorenz ratio is interpreted to mean that $N(T, c)$ is proportional to concentration in the higher ranges of concentration. A rise back towards the theoretical Lorenz number would indicate that $N(T, c)$ varies less rapidly than linearly with impurity concentration.

Daniel and Friedel[31] have proposed that in the higher ranges of impurity concentration the number of local moments in fields such that $\mu_B H \sim K_B T$ is approximately independent of concentration. This can be understood by noting that the distribution function $P(H)$ for the field experienced by a particular local moment is peaked like c^{-1} at $H = 0$ with a width proportional to c. The probability that a particular moment experiences internal fields such that $\mu_B H \sim K_B T$, and hence the total number of such moments, N, is independent of the concentration. The concentration-independent behavior of the Lorenz ratio at concentrations greater than 0.2 at.% is in disagreement with theory, since this behavior is indicative of an N proportional to c.

It is unlikely that any gross errors were made in separating the lattice conductivities as is indicated by the satisfactory agreement between the Lorenz ratios at 2 °K of annealed and unannealed samples of 0.98-at.% impurity concentration. It was concluded above that the only effect of the unannealed state of sample 11-2 was to make a temperature-independent contribution to the electrical resistivity. Any effect on the resistive anomalies was found to be unmeasurably small, indicating that the effectiveness of impurities in spin-flip exchange scattering is independent of the state of anneal. As the Lorenz ratio depends only on such scattering, it is expected that the Lorenz ratio of annealed and unannealed samples of equally concentrated samples should be similar. A significant dislocation density was found to be responsible for reducing the lattice conductivity of the unannealed specimen of the same concentration by at least a factor of 3. The observed agreement between Lorenz ratios of samples of significantly differing lattice conductivities then provides a check on the method of separation of electronic and lattice thermal conductivities and lends confidence to that separation. Satisfactory agreement is obtained between annealed and unannealed samples of 0.0273-at.% impurity concentration as well.

In the higher ranges of impurity concentration where the magnetic interaction between local moments is clearly appreciable, it is perhaps more reasonable to think of an exchange interaction between an electron and a "cluster" of local moments rather than between an electron and one local moment as has been done above. That is, the one-electron one-impurity picture inherent in the discussion to this point might be an oversimplification. In a scattering process between an electron and a cluster of impurities, the spins of the electron and of several of the members of the cluster might be flipped. The random nature of the internal field experienced by individual local moments ensures that the Zeeman splittings of the members of the cluster are likely to be different. As a result, the electron will see not just the Zeeman levels of an individual local moment but a multiplet of Zeeman levels associated with the cluster. Although many or all of the members of the cluster might be in fields $\mu_B H \gg K_B T$, the spacing of the cluster levels can be comparable to $K_B T$, enabling spin-flip inelastic electron scattering to occur even at those temperatures and concentrations where this would be forbidden on the basis of an interaction with one impurity along.

Such cooperative behavior of impurity moments could result in the continued depression of the Lorenz ratio at high concentrations. The difficulty is that it is questionable whether the RKY potential is of sufficiently long range to enable cooperative impurity-moment behavior to occur. Klein[6] has estimated that only about three or four local moments are strongly correlated to any particular local moment, even at concentrations of the order of 1 at.%. On the other hand, Overhauser[4] has proposed an additional longer-range ordering mechanism to the short-range RKY potential. At high-impurity concentrations (typically 1 at.%), he finds that it is energetically favorable for the impurity moments to interact with a static spin-density wave set up by the conduction electrons. This model differs from that of Klein insofar as the RKY interaction is replaced by a longer-range ordering mechanism, and enhancing the ability of the impurity moments to react cooperatively.

V. SUMMARY

The findings of the present study can be summarized as follows:

(i) The temperature-independent electrical resistivity due to ordinary potential and nonflip exchange scattering was found to vary as 7.50 $\mu\Omega$cm/at.%.

(ii) The variation of the slope of the linear region of the resistivity-versus-temperature curve with impurity concentration is $c^{1/5}$, in agreement with the concentration dependence of the excess low-temperature specific heat arising from the interaction between local magnetic moments associated with the iron impurities. It is not known whether this $c^{1/5}$ dependence is peculiar to the gold-iron system or is characteristic of the entire class of alloy system. Published data[1] lack the quality and/or quantity to answer this question. Measurements on the Au-Cr alloy system are in progress in this laboratory.

(iii) The temperature of the electrical resistivity maximum T_{max} varies linearly with impurity concentration in agreement with the predictions of Harrison and Klein. T_{max}/c is 24 °K/at.% iron concentration.

(iv) A comparison of the very-dilute concentration resistivity data to the theory of Kondo yields a value of the s-d exchange energy in gold-iron.

The value we obtain is $-(0.28 \pm 0.05)$ eV. It will be interesting to see how this compares to the value that will be determined for Au-Cr.

(v) The variation of the product of the electronic thermal resistivity and the temperature $W_e T$ with the temperature was found to contain a logarithmic term in the very-dilute-concentration range. The fractional magnitude of the logarithmic rise in $W_e T$ as the temperature was lowered from 4.2 to 1 °K was equal in magnitude to that of the electrical resistivity, indicating that in the very-dilute-concentration range, conduction-electron scattering is predominantly elastic.

(vi) At those impurity concentrations and temperatures where significant deviations to the Kondo $-\ln T$ behavior of the electrical resistivity are noted, the Lorenz ratio begins to decrease with decreasing temperature. This is accompanied by a decrease of the isothermal Lorenz ratio with increasing impurity concentration. This behavior persists to a concentration of about 0.2 at.% corresponding to the concentration of a sample of high enough iron content to have a Néel temperature in the liquid-helium range. At larger concentrations, of iron, the Lorenz ratio becomes constant in temperature and impurity concentration. The absence of any indication of a rise in the Lorenz ratio at the lowest temperatures and high concentrations of measurement is perhaps indicative of cooperative exchange scattering of an electron by a system of coupled impurities. The Lorenz ratio is found to be depressed to a maximum of 15% relative to the theoretical Lorenz number.

(vii) The variation of the lattice thermal conductivity with impurity concentration for Au-Fe has been established. This variation is not qualitatively different from that found by other workers for other alloy sytems.

ACKNOWLEDGMENTS

The authors wish to thank Professor P. G. Klemen, Professor R. H. Bartram, and Professor D. Markowitz for many stimulating discussions; K. Johnson, D. Strom, and D. Musante for help with the reduction of data; Mrs. Kathleen Meadows for typing the manuscript; and H. Taylor and P. Smith for technical assistance. The computational part of this work was carried out via the facilities of the Computer Center of the University of Connecticut which is supported by Grant No. GP-1819 of the National Science Foundation.

---

†Work supported by the U. S. Air Force Office of Scientific Research Grant No. AF-AFOSR-474-67 and Office of Naval Research Contract No. N00014-68-C-0491.

*Present address: International Busi..ess Machines Corporation, East Fishkill, N. Y. 12533.

[1]A good review of the literature, with an extensive bibliography, may be found in G. J. van den Berg, in *Proceedings of the Ninth International Conference on Low-Temperature Physics, Colmbus, Ohio*, edited by J. G. Daunt *el al.* (Plenum, New York, 1965), Pt. B, p. 955.

[2]J. Kondo, Progr. Theoret. Phys. (Kyoto) 32, 37 (1964).

[3]A. A. Abrikosov, Physics 2, 61 (1965).

[4]A. W. Overhauser, J. Phys. Chem. Solids 13, 71 (1959).

[5]M. W. Klein and R. Brout, Phys. Rev. 132, 2412 (1963).

[6]M. W. Klein, Phys. Rev. 136, A1156 (1964).

[7]R. J. Harrison and M. W. Klein, Phys. Rev. 154, 540 (1967).

[8]M. A. Ruderman and C. Kittel, Phys. Rev. 96, 99 (1954).

[9]K. Yosida, Phys. Rev. 106, 893 (1957).

[10]A. N. Gerritsen, Physica 25, 489 (1959).

[11]D. K. C. MacDonald, W. B. Pearson, and I. M. Templeton, Proc. Roy. Soc. (London) A266, 161 (1962).

[12]B. Dreyfus, S. Souletie, R. Tournier, and L. Weil, Compt. Rend. 259, 4266 (1964).

[13]O. S. Lutes and J. L. Schmit, Phys. Rev. 134, 676 (1964).

[14]M. S. R. Chari and J. de Nobel, Physica 25, 60 (1959).

[15]H. L. Malm and S. B. Woods, Can. J. Phys. 44, 2293 (1966).

[16]For the conditions of validity of this approximation and for a complete discussion of the lattice thermal conductivity, see P. G. Klemens, in *Handbuch der Physik*, edited by S. Flügge (Springer, Berlin, 1956), Vol. XIV, pp. 198–280.

[17]J. M. Ziman, *Principles of the Theory of Solids* (Cambridge U. P., London, 1964), pp. 198–199.

[18]Supplied by Johnson Matthey & Co. Ltd., London.

[19]Kindly supplied by Dr. T. A. Kitchens of Brookhaven National Laboratory; made at the Lawrence Radiation Laboratory by Dr. R. J. Borg.

[20]F. V. Burckbuchler and C. A. Reynolds, Phys. Rev. 175, 550 (1968).

[21]J. E. Gueths, N. N. Clark, D. Markowitz, F. V. Burckbuchler, and C. A. Reynolds, Phys. Rev. 163, 364 (1967).

[22]G. K. White, *Experimental Techniques in Low Temperature Physics* (Oxford U. P., London, 1959), p. 271.

[23]D. Shoenberg, Proc. Phys. Soc. (London) 79, 1 (1967).

[24]H. M. Rosenberg, Phil. Trans. Roy. Soc. London A247, 441 (1955).

[25]G. K. White, Proc. Phys. Soc. (London) A66, 559 (1953).

[26]G. K. White, S. B. Woods, and M. T. Elford, Phil. Mag. 4, 688 (1959).

[27]P. G. Klemens, Australian J. Phys. 7, 57 (1954).

[28]P. G. Klemens and L. Tewordt, Rev. Mod. Phys. 36, 118 (1964).

[29]W. M. Rogers and R. L. Powell, *Tables of Transport Integrals*, Natl. Bur. Std. Circular No. 595 (U. S. GPO, Washington, D. C., 1958).

[30]D. A. Spohr and R. T. Webber, Phys. Rev. 105, 1427 (1957).

[31]E. Daniel and J. Friedel, in Ref. 1, p. 933.